RESEARCH PAPER

Shaohua Chen · Tzuchiang Wang
Sharon Kao-Walter

Finite boundary effects in problem of a crack perpendicular to and terminating at a bimaterial interface*

Abstract In this paper, the problem of a crack perpendicular to and terminating at an interface in bimaterial structure with finite boundaries is investigated. The dislocation simulation method and boundary collocation approach are used to derive and solve the basic equations. Two kinds of loading form are considered when the crack lies in a softer or a stiffer material, one is an ideal loading and the other one fits to the practical experiment loading. Complete solutions of the stress field including the T stress are obtained as well as the stress intensity factors. Influences of T stress on the stress field ahead of the crack tip are studied. Finite boundary effects on the stress intensity factors are emphasized. Comparisons with the problem presented by Chen et al. (Int. J. Solids and Structure, 2003, 40, 2731–2755) are discussed also.

Keywords Bimaterial structure · Finite boundary · Crack · Stress intensity factor · T stress

1 Introduction

The influence of cracks is very important in advanced materials, such as fiber or particle reinforced composites, metal and ceramics interfaces, laminated ceramics, packaging materials and so on. Interface failures are common features in those materials and thin films. The design process of those components requires a better understanding of the failure mechanisms. One of the important tasks is to study in detail the fracture characteristics of cracks along or perpendicular to the interface.

Many researchers have investigated the interaction between an interface and a crack with various methods. Zak and Williams [1] used the eigenfunction expansion method to analyze the stress singularity at the tip of a crack, perpendicular to and terminating at the interface. Cook and Erdogan [2] used the Mellin transform method to derive the governing equation of finite cracks perpendicular to an interface and obtained the stress intensity factors. Erdogan and Biricikoglu [3] solved the problem of two bounded half planes with a crack going through the interface. Bogy [4] investigated the stress singularity of an infinite crack terminated at the interface with an arbitrary angle. Wang and Chen [5] used photoelasticity to determine the stress distribution and the stress intensity of a crack perpendicular to the interface. Wang and Stahle [6,7] used the dislocation simulation approach to investigate a crack perpendicular to and terminating at the bimaterial interface. Lin and Mar [8] presented a finite element analysis of the stress intensity factors for cracks perpendicular to the bimaterial interface. Meguid et al. [9] proposed a novel finite element to analyze edge cracks in a finite elastic homogeneous body and a finite crack perpendicular to the interface in an infinite bimaterial solid. Chen [10] used the body force to determine the stress intensity factors for a crack normal to and terminating at the bimaterial interface. Suo [11] analyzed the interaction problem of an edge dislocation with a bimaterial interface. Stahle et al. [12] investigated a crack growing towards to a bimaterial interface, where they carried out an experiment work and a finite element simulation. Recently, Leblond et al. [13] studied a crack kinking from an initially closed crack and Chen [14] investigated the T stress in plane elasticity crack problems.

The above studies are almost all about crack and interface problems in an infinite body. Few analytical solutions about interaction of a crack and an interface in a finite solid are available. In engineering applications, one has to deal with bodies with finite scales, especially the interaction of a crack and an interface in a bimaterial solid or a packaging. In 2003, Chen et al. [15] have studied the problem of a crack

S. H. Chen (✉) · T. C. Wang
LNM, Institute of Mechanics, Chinese Academy of Sciences, Beijing, 100080, China
E-mail: chenshaohua72@hotmail.com

S. Kao-Walter
Department of Mechanical Engineering, Blekinge Institute of Technology, S-371 79, Karlskrona, Sweden

perpendicular to the bimaterial interface in a finite solid but the crack tip does not reach the interface and the distance between them is b, in which the stress distributions ahead of the crack tip were shown and the stress intensity factors were given also. It was found that the finite boundaries had significant influences on the stress distributions and the stress intensity factors.

Is the present problem a special case of that investigated in [15], $i.e.$ $b = 0$? Are the stress distribution characteristics the same as those found in [15] or will the stress intensity factors in the present problem be derived as a special example of that in [15]? What about the influences of the finite boundary on the stress distributions and the stress intensity factors of this problem if it is not a special case of that? All these questions need answers. This is the reason for investigating the present problem.

The dislocation simulation method and the boundary collocation approach are used in this paper. The dislocation density is expressed as a series of the first Chebyshev polynominal with a set of unknown coefficients plus a special term. Two additional holomorphic functions are introduced in order to satisfy the outside boundary conditions. Combined with the boundary collocation method, the governing equations are solved numerically. The complete solution of the stress field and the stress intensity factors are obtained. Finite boundary effects are considered mainly. Finally, comparisons with the problem investigated in [15] are discussed.

2 Basic Equations

2.1 Complex potentials

In this section, basic equations are given for a finite crack perpendicular to the interface in an elastic body with finite boundaries. Stresses and displacements can be expressed by two Muskhelishivili's potentials:

$$\begin{cases} \sigma_x + \sigma_y = 4\mathrm{Re}\left\{\Phi(z)\right\} \\ \sigma_y - i\tau_{xy} = \Phi(z) + \Omega(\bar{z}) + (z - \bar{z})\overline{\Phi'(z)} \\ 2\mu(u_x + iu_y) = \kappa\phi(z) - \omega(\bar{z}) - (z - \bar{z})\overline{\Phi(z)} \end{cases} \quad (1)$$

where $\Phi(z) = \phi'(z)$, $\Omega(z) = \omega'(z)$.

The complex potentials for an edge dislocation at $z = s$ in an infinite elastic solid can be expressed as follows:

$$\Phi_0(z) = \frac{B}{z - s} \quad (2)$$

$$\Omega_0(z) = \frac{B}{z - \bar{s}} + \bar{B}\frac{s - \bar{s}}{(z - \bar{s})^2} \quad (3)$$

where $B = \frac{\mu}{\pi i(\kappa+1)}(b_x + ib_y)$ and b_x and b_y are the x and y components of the Burgers vector of the dislocation, $\kappa = 3 - 4\nu$ for the plane strain case and $\kappa = \frac{3-\nu}{1+\nu}$ for the plane stress case, ν and μ are Poisson's ratio and shear modulus, respectively.

Considering the interaction of an edge dislocation with a bimaterial interface, the traction and displacement continuity conditions at the interface, one can get the complex potentials for the problem of a bimaterial structure with

finite boundaries, which are similar to those for the infinite boundary problem [11]

$$\Phi(z) = \begin{cases} (1 + \Lambda_1)\Phi_0(z) + (1 + \Lambda_1)F(z) + \lambda_1 G(z) & z \in S_1 \\ \Phi_0(z) + \Lambda_2\Omega_0(z) + \lambda_2 G(z) + F(z) & z \in S_2 \end{cases} \quad (4)$$

$$\Omega(z) = \begin{cases} \Omega_0(z) + \Lambda_1\Phi_0(z) + \Lambda_1 F(z) + \lambda_1 G(z) & z \in S_1 \\ (1 + \Lambda_2)\Omega_0(z) + \lambda_2 G(z) & z \in S_2 \end{cases} \quad (5)$$

where S_1 denotes the region above the interface and S_2 is the region below the interface.

$$\lambda_1 = \frac{1}{1 - \beta} \qquad \lambda_2 = \frac{1}{1 + \beta} \quad (6)$$

$$\Lambda_1 = \frac{\alpha + \beta}{1 - \beta} \qquad \Lambda_2 = \frac{\alpha - \beta}{1 + \beta} \quad (7)$$

and α and β are two Dundurs' parameters

$$\alpha = \frac{\Gamma(\kappa_2 + 1) - (\kappa_1 + 1)}{\Gamma(\kappa_2 + 1) + (\kappa_1 + 1)} \qquad \beta = \frac{\Gamma(\kappa_2 - 1) - (\kappa_1 - 1)}{\Gamma(\kappa_2 + 1) + (\kappa_1 + 1)} \quad (8)$$

$$\Gamma = \mu_1/\mu_2 \quad (9)$$

The two holomorphic functions F, G are introduced to describe the finite boundary effects and can be expressed as follows,

$$F(z) = \sum_{n=1}^{\infty} nb_n z^{n-1} \qquad G(z) = \sum_{n=1}^{\infty} nc_n z^{n-1} \quad (10)$$

With an assumption that the crack is a continuous distribution of dislocations and lies in the lower region, we have

$$\Phi_0(z) = \frac{\mu_2}{\pi i(1 + \kappa_2)} \int_0^a \frac{(b_x + ib_y)}{z + it} \mathrm{d}t \quad (11)$$

$$\Omega_0(z) = \frac{\mu_2}{\pi i(1 + \kappa_2)} \int_0^a \frac{(b_x + ib_y)}{z - it} \mathrm{d}t + \frac{2\mu_2}{\pi(1 + \kappa_2)} \int_0^a \frac{t(b_x - ib_y)}{(z - it)^2} \mathrm{d}t \quad (12)$$

where a is the whole crack length.

According to [6,7], we introduce a new complex variable z^* and a new function $I(z^*)$

$$z^* = iz \qquad I(z^*) = \frac{1}{\pi} \int_0^a \frac{b_x + ib_y}{z^* - t} \mathrm{d}t \quad (13)$$

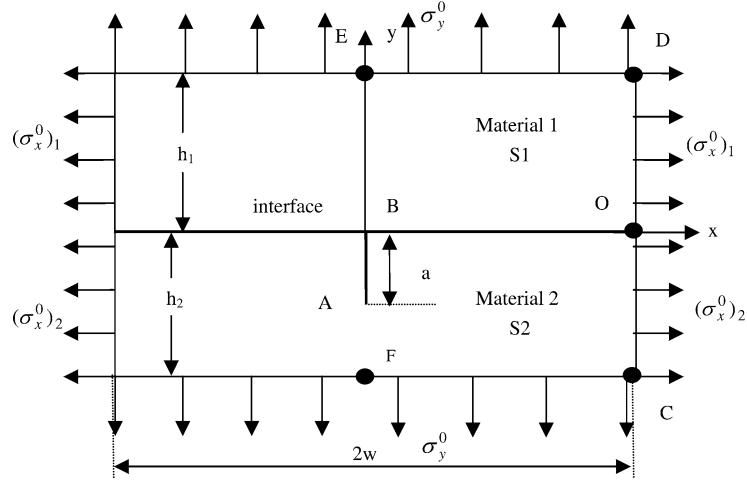Using the following variable transformations:

$$z^* = \frac{a}{2}(1 + \varsigma) \qquad t = \frac{a}{2}(1 + \xi) \quad (14)$$

The function $I(z^*)$ can be represented as

$$I(z^*) = \frac{1}{\pi} \int_{-1}^1 \frac{b_x + ib_y}{\varsigma - \xi} \mathrm{d}\xi \quad (15)$$

With the assumption that the dislocation density can be expanded as a series of the first Chebyshev polynomial plus a special term, which creates a desired stress singularity at the crack tip B as shown in Fig. 1, we can write

$$b_x + ib_y = \frac{1}{\sqrt{1 - \xi^2}} \sum_{m=0}^{\infty} \alpha_m T_m(\xi) + \beta_0 \left(\frac{1 - \xi}{1 + \xi}\right)^{\lambda_0} \quad (16)$$

Fig. 1 Scheme of a finite crack perpendicular to and terminating at a bimaterial interface in a structure with finite boundaries

where $T_m(\xi)$ is the first Chebyshev polynomial and α_m ($m = 0, \cdots\cdots, \infty$), β_0 are unknown coefficients.

$$T_m(\xi) = \cos m\theta \qquad \xi = \cos\theta \qquad (17)$$

and λ_0 is the dominating singularity, which has relation with the two Dundurs' parameters α, β and can be obtained from the following equation,

$$2(1 - \lambda_0)^2(\alpha - \beta)(1 - \beta) - \alpha - \beta^2 - (1 - \beta^2) \\ \times \cos[(1 - \lambda_0)\pi] = 0 \qquad (18)$$

The opening displacements on the crack surface can be obtained as

$$\delta_x + i\delta_y = \int_0^t (b_x + ib_y)\mathrm{d}t \\ = \int_{-1}^{\xi} \left[\frac{1}{\sqrt{1 - \xi^2}} \sum_{m=0}^{\infty} \alpha_m T_m(\xi) + \beta_0 \left(\frac{1 - \xi}{1 + \xi}\right)^{\lambda_0} \right] \\ \times \mathrm{d}\xi a_0 \\ = a_0\alpha_0(\pi - \theta) - a_0 \sum_{m=1}^{\infty} \alpha_m \frac{\sin m\theta}{m} \\ + \int_{-1}^{\xi} a_0\beta_0 \left(\frac{1 - \xi}{1 + \xi}\right)^{\lambda_0} \mathrm{d}\xi \qquad (19)$$

where a_0 is a half of the crack length. We have

$$a_0 = a/2 \qquad \xi = \cos\theta = (t - a_0)/a_0 \qquad (20)$$

At the crack tip A as shown in Fig. 1, the opening displacement should be zero and we have $t = a$, $\theta = 0$, $\xi = 1$. Then the following equation can be obtained

$$\alpha_0 + \beta_0 \frac{2\lambda_0}{\sin\pi\lambda_0} = 0 \qquad (21)$$

The above equation (21) establishes the relation between α_0 and β_0.

Using the following equation, which can be found in [16],

$$\frac{1}{\pi} \int_{-1}^1 \frac{T_m(x)}{\sqrt{1 - x^2}(z - x)}\mathrm{d}x = \frac{1}{\sqrt{z^2 - 1}} \left[z - \sqrt{z^2 - 1}\right]^m \qquad (22)$$

we obtain

$$I(z^*) = \frac{1}{\sqrt{\varsigma^2 - 1}} \sum_{m=0}^{\infty} \alpha_m \left[\varsigma - \sqrt{\varsigma^2 - 1}\right]^m \\ - \frac{\beta_0}{\sin\pi\lambda_0} \left[\left(\frac{\varsigma - 1}{\varsigma + 1}\right)^{\lambda_0} - 1\right] \qquad (23)$$

$$\varsigma = \frac{z^*}{a_0} - 1 \qquad (24)$$

2.2 Stress jump across the interface

We know that the displacements should be continuous across the interface and the strain ε_x should be continuous across the interface also. It follows that

$$(\varepsilon_x)_1 = (\varepsilon_x)_2 \quad \text{on the interface} \qquad (25)$$

For the plane strain problem, the above equation can be written as

$$(\sigma_x)_1 = \frac{(1 + \alpha)}{(1 - \alpha)}(\sigma_x)_2 + \frac{2\sigma_y}{1 - \alpha}(2\beta - \alpha) \\ \text{on the interface} \qquad (26)$$

We assume that the external loading satisfies equation (26), so

$$(\sigma_x^0)_1 = \frac{(1 + \alpha)}{(1 - \alpha)}(\sigma_x^0)_2 + \frac{2\sigma_y^0}{1 - \alpha}(2\beta - \alpha) \qquad (27)$$

where $(\sigma_x^0)_1$ and $(\sigma_x^0)_2$ are the external loading acted on the outside vertical boundaries of materials 1 and 2 in the direction of x axis, respectively. σ_y^0 is the external loading acted on

on the upper and lower boundaries in the direction of y axis. It should be noted that if this assumption is not adopted, the energy method can be used to analyze this problem but the numerical calculation can be very complex. Using this assumption, the whole field can be looked as a homogeneous field without a crack plus a perturbation field and the boundary collocation method will have high precision for this kind of field.

In the present paper, two kinds of loading form are considered and we call them case I and case II.

2.3 Governing equations for case I

The problem of case I is shown in Fig.1, in which $(\sigma_x^0)_1$ is loaded on the right and left boundaries of the upper region S_1 and $(\sigma_x^0)_2$ is loaded on the right and left boundaries of the lower region S_2. In this case, $\sigma_y^0 = 0$, then the relation between $(\sigma_x^0)_1$ and $(\sigma_x^0)_2$ becomes

$$(\sigma_x^0)_1 = \frac{(1+\alpha)}{(1-\alpha)}(\sigma_x^0)_2 \qquad (28)$$

The crack lies in the lower region S_2 and the crack length is $2a_0$. The crack tip point B is terminating at the interface. The width of the structure is $2w$ and the height of the upper region is h_1 and that of the lower region is h_2. Both the upper and lower materials are elastic.

Superposition scheme is used. The first solution is for the bimaterial without crack subject to a uniform external loading on the vertical outside boundaries, which can be written as,

$$\sigma_x = (\sigma_x^0)_1 \qquad \sigma_y = \sigma_y^0 = 0 \qquad \tau_{xy} = 0$$
$$\text{in material 1} \qquad (29)$$

$$\sigma_x = (\sigma_x^0)_2 \qquad \sigma_y = \sigma_y^0 = 0 \qquad \tau_{xy} = 0$$
$$\text{in material 2} \qquad (30)$$

The second solution is for a crack perpendicular to and terminating at the interface with a uniform traction prescribed on the crack faces and traction free on the outside boundaries. So we have the following equation for the crack face,

$$\sigma_x + i\tau_{xy} = \Phi(z) + 2\overline{\Phi(z)} - \Omega(\bar{z}) - (z - \bar{z})\overline{\Phi'(z)}$$
$$= -\sigma \qquad z = \pm 0 + iy, \quad -a < y < 0 \quad (31)$$

where

$$\sigma = (\sigma_x^0)_2 \qquad (32)$$

Due to the symmetry, $b_y = 0$, we obtain

$$\Phi_0(z) = \frac{\mu_2}{(\kappa_2 + 1)} I(iz) \qquad (33)$$

$$\Omega_0(z) = \frac{\mu_2}{(\kappa_2 + 1)} I(-iz) - \frac{2\mu_2}{(\kappa_2 + 1)} iz I'(-iz) \qquad (34)$$

Substituting equations (4, 5, 10, 33, 34) into (31), we obtain the following traction equation on the crack face,

$$\frac{\mu_2}{\kappa_2 + 1}\left\{ 2\overline{I^+(t)} + 2t\left[\overline{I'^+(t)} - I'^-(t)\right] + I^+(t) - I^-(t)\right.$$

$$\left. + (3\Lambda_2 - \Lambda_1)I(-t) - 12\Lambda_2 t I'(-t) + 4t^2\Lambda_2 I''(-t)\right\}$$

$$+ \sum_{n=1}^{\infty} n(b_n + \lambda_2 c_n)z^{n-1} + 2\sum_{n=1}^{\infty} n(\bar{b}_n + \lambda_2\bar{c}_n)\bar{z}^{n-1}$$

$$- \lambda_1 \sum_{n=1}^{\infty} n c_n \bar{z}^{n-1} - \Lambda_1 \sum_{n=1}^{\infty} n b_n \bar{z}^{n-1}$$

$$+ 2\sum_{n=1}^{\infty} n(n-1)(\bar{b}_n + \lambda_2\bar{c}_n)\bar{z}^{n-1} = -\sigma \qquad (35)$$

where $0 < t < a$.

The governing equation for the present problem contains a set of unknown coefficients α_m ($m = 0, \cdots, \infty$), β_0, b_n and c_n ($n = 1, \cdots, \infty$). It is difficult to solve the governing equations analytically. Boundary collocation method will be used and resultant forces on outside boundaries are used as the boundary conditions. Point O is assumed to be fixed at all times as shown in Fig. 1, a point C^* is permitted to move along the outside edge. Boundary conditions can be written as follows:

$$C^* \in \text{OCF}: \qquad X + iY = 0 \qquad (36)$$
$$C^* \in \text{ODE}: \qquad X + iY = 0 \qquad (37)$$

The resultant forces from O to C^* can be expressed as

$$X(z) + iY(z) = -i\left[\phi(z) + \omega(\bar{z}) + (z - \bar{z})\overline{\Phi(z)}\right]^{C^*} \qquad (38)$$

During the solving process, the crack surface will be divided into M elements and the nodal points are given by the following expression:

$$t_k = a_0 + a_0 \cos\theta_k \qquad \theta_k = \frac{k\pi}{(M+1)} \quad k = 1, 2, \ldots, M \qquad (39)$$

The i-th outer edge of the rectangular plate is divided regularly into N_i ($i = 1, 2, 3, 4$) segments.

2.4 Governing equations for case II

The problem of case II with different loading form from case I fits to the practical experiment loading and a homogeneous stress $(\sigma_x^0)_1 = (\sigma_x^0)_2 = \sigma$ is loaded on the left and right edges, on the upper and lower edges is a homogeneous stress loading σ_y^0, where equation (27) is still satisfied. The crack face is traction free. The governing equation on the crack face for case II is

$$\frac{\mu_2}{\kappa_2+1}\left\{2\overline{I^+(t)}+2t\left[\overline{I'^+(t)}-I'^-(t)\right]+I^+(t)-I^-(t)\right.$$

$$\left.+(3\Lambda_2-\Lambda_1)I(-t)-12\Lambda_2tI'(-t)+4t^2\Lambda_2I''(-t)\right\}$$

$$+\sum_{n=1}^{\infty}n(b_n+\lambda_2c_n)z^{n-1}+2\sum_{n=1}^{\infty}n(\bar{b}_n+\lambda_2\bar{c}_n)\bar{z}^{n-1}$$

$$-\lambda_1\sum_{n=1}^{\infty}nc_n\bar{z}^{n-1}-\Lambda_1\sum_{n=1}^{\infty}nb_n\bar{z}^{n-1}$$

$$+2\sum_{n=1}^{\infty}n(n-1)(\bar{b}_n+\lambda_2\bar{c}_n)\bar{z}^{n-1}=0 \qquad (40)$$

where $0 < t < a$.

For case II, point O is assumed to be fixed at all times, a point C^* is permitted to move along the outside edge, which is similar to case I. Boundary conditions are written in terms of the resultant forces from O to C^* as follows:

$$\begin{array}{ll} C^* \in OC: & X+iY=\sigma y \\ C^* \in CF: & X+iY=-\sigma h_2+i\sigma_y^0(w-x) \\ C^* \in OD: & X+iY=\sigma y \\ C^* \in DE: & X+iY=\sigma h_1+i\sigma_y^0(w-x) \end{array} \qquad (41)$$

Boundary collocation method will also be used to solve the governing equation (40) for case II.

2.5 Stress Intensity factor

The stress components ahead of the crack tip B can be expressed as follows

$$\sigma_x=\frac{\mu_2}{\kappa_2+1}\left[(2+3\Lambda_1-\Lambda_2)I(t)+2(\Lambda_1-\Lambda_2)tI'(t)\right]$$

$$+\sum_{n=1}^{\infty}n[(1+\Lambda_1)b_n+\lambda_1c_n]z^{n-1}$$

$$+2\sum_{n=1}^{\infty}n[(1+\Lambda_1)\bar{b}_n+\lambda_1\bar{c}_n]\bar{z}^{n-1}$$

$$-\lambda_2\sum_{n=1}^{\infty}nc_n\bar{z}^{n-1}$$

$$+2\sum_{n=1}^{\infty}n(n-1)[(1+\Lambda_1)\bar{b}_n+\lambda_1\bar{c}_n]\bar{z}^{n-1} \qquad (42)$$

and

$$\sigma_y=\frac{\mu_2}{\kappa_2+1}\left[(2+\Lambda_2+\Lambda_1)I(t)-2(\Lambda_1-\Lambda_2)tI'(t)\right]$$

$$+\sum_{n=1}^{\infty}3(1+\Lambda_1)nb_nz^{n-1}+\sum_{n=1}^{\infty}3\lambda_1nc_nz^{n-1}$$

$$-2\sum_{n=1}^{\infty}n[(1+\Lambda_1)\bar{b}_n+\lambda_1\bar{c}_n]\bar{z}^{n-1}+\lambda_2\sum_{n=1}^{\infty}nc_n\bar{z}^{n-1}$$

$$-2\sum_{n=1}^{\infty}n(n-1)[(1+\Lambda_1)\bar{b}_n+\lambda_1\bar{c}_n]\bar{z}^{n-1} \qquad (43)$$

On the right side of Equations (42) and (43), the function $I(t)$ can be expanded as

$$I(t)=\frac{1}{\sqrt{\xi^2-1}}\sum_{m=0,1}^{\infty}\alpha_m\left[\xi-\sqrt{\xi^2-1}\right]^m$$

$$-\frac{\beta_0}{\sin\pi\lambda_0}\left[\left(\frac{\xi-1}{\xi+1}\right)^{\lambda_0}-1\right] \qquad (44)$$

If $\lambda_0 > 0.5$, the strongest stress singularity is produced by the special term, which is related to the parameter β_0. The stresses near the crack tip B can be represented as

$$\sigma_{ij}=\frac{Q_I}{(2\pi r)^{\lambda_0}}f_{ij}(\theta) \qquad (45)$$

where Q_I is the generalized stress intensity factor for this interface problem. One can obtain

$$Q_I=\lim_{r\to 0}(2\pi r)^{\lambda_0}\sigma_x$$

$$=-\frac{\beta_0\mu_2}{(k_2+1)\sin\pi\lambda_0}(2\pi a_0)^{\lambda_0}2^{\lambda_0}[(2+3\Lambda_1-\Lambda_2)$$

$$-2(\Lambda_1-\Lambda_2)\lambda_0] \qquad (46)$$

The dominating singular field (Q field) can be obtained from Equations (42) and (43) as

$$\sigma_x^Q=-\frac{\beta_0\mu_2}{(k_2+1)\sin\pi\lambda_0}(2\pi a_0)^{\lambda_0}2^{\lambda_0}$$

$$\times[(2+3\Lambda_1-\Lambda_2)-2(\Lambda_1-\Lambda_2)\lambda_0](2\pi r)^{-\lambda_0} \quad (47)$$

and

$$\sigma_y^Q=-\frac{\beta_0\mu_2}{(k_2+1)\sin\pi\lambda_0}(2\pi a_0)^{\lambda_0}2^{\lambda_0}$$

$$\times[(2+\Lambda_1+\Lambda_2)+2(\Lambda_1-\Lambda_2)\lambda_0](2\pi r)^{-\lambda_0} \quad (48)$$

The normal stress ahead of the crack tip B can be rewritten as

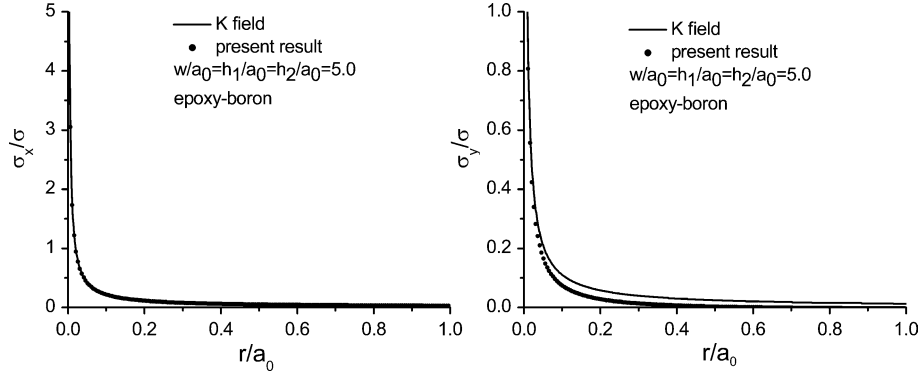$$\sigma_x=\frac{Q_I}{(2\pi r)^{\lambda_0}}f_x(\theta)+\sigma_x^* \qquad (49)$$

For stress σ_x^*, we have

$$\lim_{r\to 0}\sqrt{2\pi r}\sigma_x^*=-\frac{2\mu_2}{(k_2+1)}(1+\Lambda_1)\sqrt{\pi a_0}$$

$$\times\sum_{m=0}^{\infty}(-1)^m\alpha_m \qquad (50)$$

Obviously, singularity of 1/2 should be excluded. It follows that

$$\sum_{m=0}^{\infty}(-1)^m\alpha_m=0 \qquad (51)$$

Fig. 2 Normalized stress distributions ahead of the crack tip B versus r/a_0 for a finite epoxy-boron bimaterial structure with case I loading form

2.6 T stress

The T stress is the second term of the Williams series. Linear elastic fracture mechanics is usually based on the assumption that the stress field near the crack tip is K field. However, much work has shown that the stress intensity factor alone might not suffice to characterize the crack tip fields. T_x is the x-component of the T stresses. For case I, T_x and T_y stresses can be obtained as follows,

$$T_x = \frac{\mu_2}{\kappa_2 + 1}(2 + 3\Lambda_1 - \Lambda_2)\left[\sum_{m=0}^{\infty}(-1)^m m\alpha_m + \frac{\beta_0}{\sin \pi \lambda_0}\right]$$
$$+ 3(1 + \Lambda_1)b_1 + (3\lambda_1 - \lambda_2)c_1 + \frac{1 + \alpha}{1 - \alpha}\sigma \qquad (52)$$

$$T_y = \frac{\mu_2}{\kappa_2 + 1}(2 + \Lambda_1 + \Lambda_2)\left[\sum_{m=0}^{\infty}(-1)^m m\alpha_m + \frac{\beta_0}{\sin \pi \lambda_0}\right]$$
$$+ (1 + \Lambda_1)b_1 + (\lambda_1 + \lambda_2)c_1 \qquad (53)$$

For case II, T_x and T_y stresses are

$$T_x = \frac{\mu_2}{\kappa_2 + 1}(2 + 3\Lambda_1 - \Lambda_2)\left[\sum_{m=0}^{\infty}(-1)^m m\alpha_m + \frac{\beta_0}{\sin \pi \lambda_0}\right]$$
$$+ 3(1 + \Lambda_1)b_1 + (3\lambda_1 - \lambda_2)c_1 \qquad (54)$$

$$T_y = \frac{\mu_2}{\kappa_2 + 1}(2 + \Lambda_1 + \Lambda_2)\left[\sum_{m=0}^{\infty}(-1)^m m\alpha_m + \frac{\beta_0}{\sin \pi \lambda_0}\right]$$
$$+ (1 + \Lambda_1)b_1 + (\lambda_1 + \lambda_2)c_1 \qquad (55)$$

3 Numerical Calculation Results

Boundary collocation method is used in this section. In order to verify our numerical program, the problem with an infinite boundary, i.e., $b_n = c_n = 0$, is calculated first, with the loading form the same as that in case I. A typical example for epoxy-boron bimaterial in the case of plane strain was tested. The coefficient α_m approaches to zero rapidly as m increases. All the calculation results for an infinite bimaterial problem are consistent with those given by [7].

3.1 The results for case I

Figure 2 shows the stress distributions ahead of the crack tip B versus the normalized distance, r/a_0, for epoxy-boron bimaterial structure. The Poisson's ratio of epoxy is $\nu_1 = 0.35$ and that of boron is $\nu_2 = 0.3$. Shear modulus ratio of the two materials is $\mu_1/\mu_2 = 0.00722$, which means that the crack lies in the stiff material. The normalized parameters are $w/a_0 = 5.0$, $h_1/a_0 = h_2/a_0 = 5.0$. From Fig. 2, we see that the Q field can characterize the normal stress field in x direction very well in the region of $0 < r/a_0 < 1.0$ and the Q field can describe adequately the normal stress field in y direction in the region of $0 < r/a_0 < 0.05$. Combining the results of the infinite boundary problem, one can find that the Q field is consistent with the normal stress field in x direction in the region of $0 < r/a_0 < 1.0$ and the Q field can describe the normal stress field in y direction in a smaller region of $0 < r/a_0 < 0.05$ either for an infinite boundary or for a finite boundary problem.

When the crack lies in a soft material (crack is always assumed in the lower material), we give the corresponding normalized stress distributions versus the normalized distance r/a_0, for a sample with the same boundary scale, i.e. $w/a_0 = 5.0$, $h_1/a_0 = h_2/a_0 = 5.0$ as those used in Fig. 2, but one should note now that the upper material is stiffer than the lower material. Fig. 3 shows the normalized stress distributions for boron-epoxy and the shear modulus ratio is $\mu_1/\mu_2 = 138.46$. From Fig. 3 one can see that the Q field is remarkably deviated from the normal stress σ_x and the Q field plus T_x stress field gives a good prediction for normal stress σ_x in the region of $0 < r/a_0 < 1.0$. It clearly shows that T_x stress has a tremendous contribution to the normal stress σ_x. The Q field plus the T_y stress also gives a good prediction for stress σ_y in the region of $0 < r/a_0 < 0.4$. The phenomena found in the infinite structure can also be found in the finite boundary sample, only the values of stresses near the crack tip are different in the two problems.

Table 1 shows the normalized stress intensity factors $\sqrt{2}Q_I/\sigma(2\pi a_0)^{\lambda_0}$ versus different shear modulus ratios, for several samples with different boundary lengths. The crack lies in material 2 and material 2 is assumed to be softer than material 1 in this case. The other parameters are $\nu_1 = 0.3$,
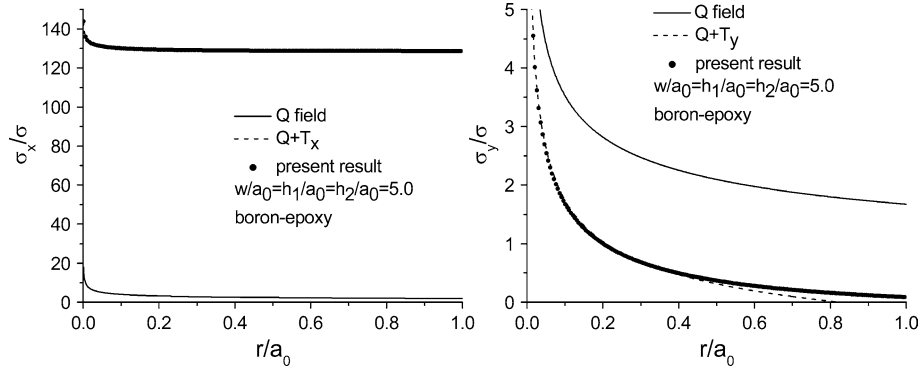
Fig. 3 Normalized stress distributions ahead of the crack tip B versus r/a_0 for a finite boron-epoxy bimaterial structure with case I loading form

Table 1 $\sqrt{2}Q_I/\sigma(2\pi a_0)^{\lambda_0}$ for case I and crack lies in a soft material 2 ($\upsilon_1 = 0.3$, $\upsilon_2 = 0.35$)

μ_1/μ_2	1000.0	500.0	250.0	100.0	50.0	10.0	5.0	1.0
$w/a_0 = 5$ $h_1/a_0 = 5$ $h_2/a_0 = 5$	2.713	2.711	2.707	2.691	2.652	2.285	1.940	1.050
$w/a_0 = 10$ $h_1/a_0 = 10$ $h_2/a_0 = 10$	2.833	2.829	2.822	2.796	2.745	2.324	1.945	0.963
$w/a_0 = 15$ $h_1/a_0 = 15$ $h_2/a_0 = 15$	2.914	2.910	2.899	2.866	2.806	2.350	1.960	0.940
Infinite solid	3.154	3.145	3.127	3.072	2.985	2.444	2.008	0.907

Table 2 $\sqrt{2}Q_I/\sigma(2\pi a_0)^{\lambda_0}$ for case I and crack lies in a stiff material 2 ($\upsilon_1 = 0.35$, $\upsilon_2 = 0.3$)

μ_1/μ_2	0.001	0.002	0.004	0.01	0.02	0.1	0.2	1.0
$w/a_0 = 5$ $h_1/a_0 = 5$ $h_2/a_0 = 5$	0.0062	0.012	0.024	0.055	0.103	0.370	0.573	1.27
$w/a_0 = 10$ $h_1/a_0 = 10$ $h_2/a_0 = 10$	0.0035	0.0070	0.013	0.032	0.061	0.248	0.421	1.17
$w/a_0 = 15$ $h_1/a_0 = 15$ $h_2/a_0 = 15$	0.0032	0.0062	0.012	0.029	0.055	0.225	0.388	1.145
Infinite solid	0.0028	0.0056	0.011	0.026	0.049	0.199	0.348	1.10

$\upsilon_2 = 0.35$, $\sigma = (\sigma_x^0)_2$. From Table 1, one can see that, for the same shear modulus ratio and $\mu_1/\mu_2 \neq 1$, the normalized stress intensity factor at crack tip B will decrease when the size of the sample decreases. The normalized stress intensity factor is the largest in the infinite-boundary problem. With the same sample size, the stress intensity factor at B will increase when the shear modulus ratio μ_1/μ_2 increases. But one should note, in this case, if we use $(\sigma_x^0)_1$ to normalize the stress intensity, all the phenomena will be inversed.

Table 2 shows the normalized stress intensity factor $\sqrt{2}Q_I/\sigma(2\pi a_0)^{\lambda_0}$ versus different shear modulus ratios for four samples with different boundary lengths and, here, the crack lies in material 2 and material 2 is assumed to be stiffer than material 1 in this case. The other parameters are $\upsilon_1 = 0.35$, $\upsilon_2 = 0.3$, $\sigma = (\sigma_x^0)_2$. From table 2, one can

also see that, for the same material pairs, the stress intensity factor will increase when the size of the sample decreases. The stress intensity factor is the smallest for the infinite problems. When the sample size is fixed, the stress intensity factor will increase as the shear modulus ratio μ_1/μ_2 increases. Also, if we use $(\sigma_x^0)_1$ to normalize the stress intensity, all the phenomena will be inversed.

3.2 The results for case II

In this sub-Sect., only the loading form is different from that in sub-Sect., 3.1, that is, $(\sigma_x^0)_1 = (\sigma_x^0)_2 = \sigma$ and σ_y^0 does not vanish. The relation between σ and σ_y^0 satisfies Eq. (27).

Figure 4 shows the stress distributions ahead of the crack tip B versus the normalized distance, r/a_0, for epoxy-boron, which means that the crack lies in a stiff material. The normalized parameters are $w/a_0 = 5.0$, $h_1/a_0 = h_2/a_0 = 5.0$. From Fig. 4, one can see that the Q field can not describe adequately the normal stress field in x direction any more, and both Q field and T_x stress should be considered in order to be consistent with the normal stress field σ_x and the region is $0 < r/a_0 < 1.0$. The Q field also can not describe the normal stress field in y direction and the Q field plus T_y stress will be consistent well with the normal stress field σ_y in the region of $0 < r/a_0 < 0.05$.

When the crack lies in a soft material, we plot the relation curves of the corresponding normalized stress distributions versus the normalized distance r/a_0, for $w/a_0 = 5.0$, $h_1/a_0 = h_2/a_0 = 5.0$. Fig. 5 shows the normalized stress distributions for boron-epoxy. In Fig. 5, one can see that the Q field is remarkably deviated from the normal stress σ_x and the Q field plus T_x stress field gives a good prediction for normal stress σ_x in the region of $0 < r/a_0 < 0.2$. The Q field gives a good prediction for stress σ_y in the region of $0 < r/a_0 < 0.4$.

Table 3 shows the normalized stress intensity factors $\sqrt{2}Q_I/\sigma(2\pi a_0)^{\lambda_0}$ versus different shear modulus ratios for different sample scales. The crack lies in a soft material 2 and $\upsilon_1 = 0.3$, $\upsilon_2 = 0.35$. One can see from table 3 that, for the same shear modulus ratio and $\mu_1/\mu_2 \neq 1$, the normalized stress intensity factor will decrease when the size of
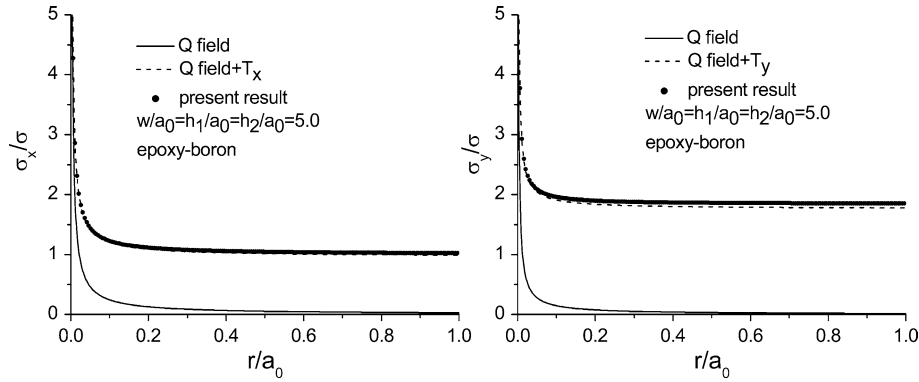
Fig. 4 Normalized stress distributions ahead of the crack tip B versus r/a_0 for a finite epoxy-boron bimaterial structure with case II loading form
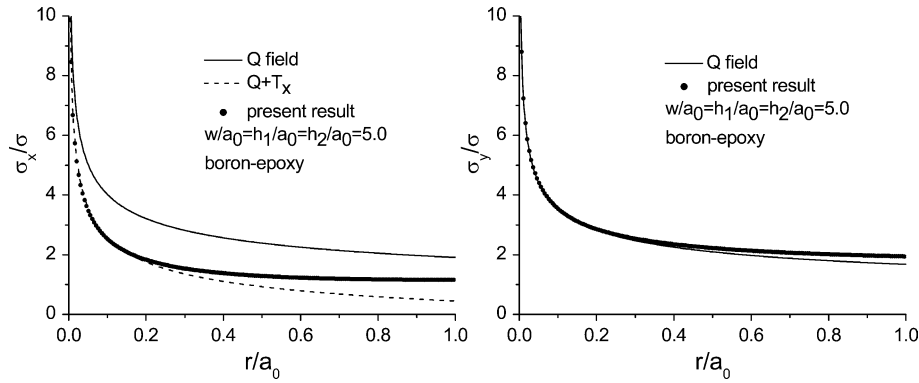

Fig. 5 Normalized stress distributions ahead of the crack tip B versus r/a_0 for a finite boron-epoxy bimaterial structure with case II loading form

Table 3 $\sqrt{2}Q_I/\sigma(2\pi a_0)^{\lambda_0}$ for case II and crack lies in a soft material 2 ($\upsilon_1 = 0.3$, $\upsilon_2 = 0.35$)

μ_1/μ_2	1000.0	500.0	250.0	100.0	50.0	10.0	5.0	1.0
$w/a_0 = 5$ $h_1/a_0 = 5$ $h_2/a_0 = 5$	2.713	2.711	2.700	2.690	2.650	2.280	1.940	1.050
$w/a_0 = 10$ $h_1/a_0 = 10$ $h_2/a_0 = 10$	2.832	2.830	2.822	2.796	2.745	2.323	1.945	0.963
$w/a_0 = 15$ $h_1/a_0 = 15$ $h_2/a_0 = 15$	2.914	2.909	2.900	2.866	2.806	2.353	1.958	0.940

Table 4 $\sqrt{2}Q_I/\sigma(2\pi a_0)^{\lambda_0}$ for case II and crack lies in a stiff material 2 ($\upsilon_1 = 0.35$, $\upsilon_2 = 0.3$)

μ_1/μ_2	0.001	0.002	0.004	0.01	0.02	0.1	0.2	1.0
$w/a_0 = 5$ $h_1/a_0 = 5$ $h_2/a_0 = 5$	0.0062	0.0122	0.0236	0.0553	0.103	0.370	0.573	1.273
$w/a_0 = 10$ $h_1/a_0 = 10$ $h_2/a_0 = 10$	0.0035	0.0069	0.0136	0.0324	0.0615	0.248	0.421	1.170
$w/a_0 = 15$ $h_1/a_0 = 15$ $h_2/a_0 = 15$	0.0032	0.0062	0.0121	0.0289	0.055	0.225	0.388	1.145

the sample decreases. For samples with the same scales, the stress intensity factor will increase when the shear modulus ratio of the stiff material to the soft material increases.

Table 4 shows the normalized stress intensity factor $\sqrt{2}Q_I/\sigma(2\pi a_0)^{\lambda_0}$ versus different shear modulus ratios for different sample scales. The crack lies in a stiff material 2 and $\nu_1 = 0.35$, $\nu_2 = 0.3$. One can also see that, for the same shear modulus ratio, the stress intensity factor will increase when the size of a sample decreases. The stress intensity factor will increase when the shear modulus ratio of the soft material to the stiff material increases for the same sample scale.

Comparing table 1 and table3, table 2 and table 4, one can see that the normalized stress intensity has no relation with the two kinds of loading forms.

From table 3 and 4, one will see, for the same sample size and $\mu_1/\mu_2 = 1$, the Poisson's ratio has influence on the stress intensity factor. This conclusion can also be made when we compare table 1 and table 2 for the case of $\mu_1/\mu_2 = 1$.

4 Comparisons with the problem in [15]

In [15], the problem of a crack perpendicular to a bimaterial interface in a finite solid was investigated. In that problem, the crack tip does not reach the bimaterial interface, *i.e.*, all the crack lies in one region, the singularity at the crack tip is always $-1/2$ and we call the elastic field as K field. While in the present paper, the crack perpendicular to and terminat-

ing at the bimaterial interface, the singularity at the crack tip is $-\lambda_0$, which is related with the two Dundur's parameters α and β. For different material pairs, the singularity varies, so we call the elastic filed as Q field.

The problem in the present paper looks like a special case of that in [15], however it is not true. If we take $b = 0$ in [15], the deduced results will be wrong, from where one can find the difference between the two kinds of problems. This conclusion is consistent with that in [9], in which the authors used finite element method and found that the results for $b = 0$ are not consistent with the results for $b \to 0$.

Since the crack lies in one region and does not reach the bimaterial interface in [15], the interesting domain of the stress distributions near the crack tip is the same as where the crack lies. While in the present paper, the crack tip lies at the bimaterial interface, the corresponding stresses that are significant for our research are the stresses in the other region comparing to the crack position.

In a whole, we can not regard the present problem as a special case of that in [15]. The present problem is often met in engineering field, which is solved analytically in the present paper.

5 Conclusions

In the present paper, the problem of a finite crack perpendicular to and terminating at the finite bimaterial interface is investigated analytically using the dislocation simulation and boundary collocation approaches. Two kinds of loading form are considered, one is an ideal loading and the other adapts to the practical experiment loading.

Different loading forms and the shear modulus ratio will influence the effective regions, in which the asymptotic Q field or the asymptotic Q field plus the T field could represent the stress field near the crack tip. Details are as follows.

In an ideal loading case (case I), when the crack lies in a stiff material, the normal stress σ_x ahead of the crack tip B, is characterized by the Q field in the region of $0 < r/a_0 < 1.0$ and the normal stress σ_y, which is parallel to the crack surface, is dominated by the Q field in the region of $0 < r/a_0 < 0.05$.

In the ideal loading case (case I), when the crack lies in a soft material, the normal stress σ_x and σ_y are dominated by the Q field plus the T stress in the region of $0 < r/a_0 < 1.0$ and $0 < r/a_0 < 0.4$.

For case II, when the crack lies in a stiff material, the Q fields deviate remarkably from the normal stress σ_x and σ_y, which are dominated by the Q field plus the T stress in the region of $0 < r/a_0 < 1.0$ and $0 < r/a_0 < 0.05$, respectively.

For case II, when the crack lies in a soft material, the normal stress σ_x is dominated by the Q field plus the T stress in the region of $0 < r/a_0 < 0.2$ and the normal stress σ_y can be described by the Q field in the region of $0 < r/a_0 < 0.4$.

In both case I and case II, when the crack lies in a stiff material, with a fixed shear modulus ratio but $\mu_1/\mu_2 \neq 1$, the normalized stress intensity factor $\sqrt{2}Q_I/\sigma(2\pi a_0)^{\lambda_0}$ at the crack tip lying on the interface (point B) will decrease as the size of the sample decreases. When the crack lies in a soft material, with a fixed shear modulus ratio, the stress intensity factor will increase as the size of the sample decreases.

In both case I and case II, when the crack lies in a soft material, with a fixed sample scale, the normalized stress intensity factor $\sqrt{2}Q_I/\sigma(2\pi a_0)^{\lambda_0}$ at crack tip (point B) will increase as the ratio of the shear modulus of the stiff material to that of the soft material increases. When the crack lies in a stiff material, with a fixed sample scale, the normalized stress intensity factor will increase as the ratio of the shear modulus of the soft material to the stiff material increases.

The two loading forms in the present paper do not influence the normalized stress intensity factor $\sqrt{2}Q_I/\sigma(2\pi a_0)^{\lambda_0}$, but Poisson's ratio does.

References

1. Zak, A.R., Williams, M.L.: Crack point singularities at a bimaterial interface. J. Appl. Mech. (**30**), 142–143 (1963)
2. Cook, T.S., Erdogan, F.: Stress in bounded material with a crack perpendicular to the interface. Int. J. Engng. Sci. (**10**), 677–697 (1972)
3. Erdogan, F., Biricikoglu, B.: Two bonded half plane with a crack through the interface. Int. J. Engng. Sciences. **11**, 745–766 (1973)
4. Bogy, D.B.: On the plane elastic problem of a loaded crack terminating a material interface. Int. J. Fract. **38**, 911–918 (1971)
5. Wang, W.C., Chen, J.T.: Theoretical and experimental re-examination of a crack at a bimaterial interface. J. Strain Analysis **28**, 53–61 (1993)
6. Wang, T.C., Stahle, P.: Stress state in front of a crack perpendicular to bimaterial interface. Engng. Fract. Mech. **59**, 471–485 (1998)
7. Wang, T.C., Stahle, P.: A crack perpendicular to and terminating at a bimaterial interface. Acta. Mech. Sinica **14**, 27–36 (1998)
8. Lin, K.Y., Mar, J.W.: Finite element analysis of a stress intensity factors for crack at a bimaterial interface. Int. J. Fract. **12**, 521–531 (1976)
9. Meguid, S.A., Tan, M., Zhu, Z.H.: Analysis of crack perpendicular to bimaterial interface using a novel finite element. Int. J. Fract. **75**, 1–25 (1995)
10. Chen, D.H.: A crack normal to and terminating at a bimaterial interface. Engng. Fract. Mech. **49**, 517–523 (1994)
11. Suo, Z.G.: Singularities interacting with interface and cracks. Int. J. Solids Struct. **25**, 1133–1142 (1989)
12. Stahle, P., Jens, G., Delfin, P.: Crack path in a weak elastic layer covering a beam. Acta. Mech. Solida Sinica **8**, 579–583 (1995)
13. Leblond, J.B., Frelat, J.: Crack kinking from an initially closed crack. Int. J. Solids Struct. **37**, 1595–1614 (2000)
14. Chen, Y.Z.: Closed form solutions of T-stress in plane elasticity crack problems. Int. J. Solids Struct. **37**, 1629–1637 (2000)
15. Chen, S.H., Wang, T.C., Kao-Walter, S.: A crack perpendicular to the bimaterial interface in finite solid. Int. J. Solids Struct. **40**, 2731–2755 (2003)
16. Gladwell, G.M.L.: Contact problem in the classical theory of elasticity. Sijthoff & Noordhoff, 1980, pp. 61–64